Arabian Journal of Geosciences (2019) 12: 258
https://doi.org/10.1007/s12517-019-4421-1

ORIGINAL PAPER

Structural properties of unsaturated compacted loess for various sample moisture contents

Yan-zhou Hao [1] · Tie-hang Wang [1] · Juan-juan Wang [1]

Received: 17 July 2018 / Accepted: 20 February 2019 / Published online: 3 April 2019

Abstract

This paper investigates the structural properties of compacted loess by focusing on the influence of structural changes incurred by varying sample moisture content on matric suction and stress-strain characteristics of unsaturated compacted loess. Two tests are conducted on unsaturated compacted loess with different structural properties: soil-water characteristic curve test and triaxial shear test. Samples are maintained and tested at the same moisture content and dry density through humidification or dehumidification. Test results show that structural changes incurred by sample moisture content markedly influence the soil-water characteristic curve of unsaturated compacted loess. Below the plastic limit, matric suction increases with increasing sample moisture content. At the optimal sample moisture content, unsaturated compacted loess exhibits a homogeneous micro-pore aggregation structure and thus a relatively high suction. In the optimal structural state, the stress-strain curve was located at the top of the stress-strain graph. For moisture contents below the optimal sample moisture content, the degree of structural weakening is relatively low, and the stress-strain curve gradually moves down the stress-strain graph. For moisture content above the optimal sample moisture content, the degree of structural weakening of the soil sample is relatively high, and the stress-strain curve moves to the bottom of the stress-strain graph. A structural parameter $m_{\varepsilon r}$ is defined that could reasonably reflect the structural properties of compacted loess and is of great significance for evaluating the engineering quality of compacted loess.

Keywords Compacted loess · Sample moisture content · Matric suction · Stress-strain curve · Structural parameter

Introduction

Loess is a special type of geological formation that is mainly distributed in mid-latitude arid and semi-arid regions in China, and its unique genesis results in unique structural properties. The importance of the structural properties of loess, which influence engineering quality, has been universally acknowledged and is deemed as a core issue of soil mechanics in the twenty-first century (Shen 1996). The method of releasing structural potential has been used to establish multiple quantitative structural parameters for undisturbed soil. The comprehensive structural potential as a soil structural parameter was introduced, and a new approach was proposed to investigate the structural properties of loess (Xie and Qi 1999). The difference in principal stresses was used to define a structural quantitative parameter for undisturbed soil, so as to reflect soil structural changes under disturbing, soaking, and loading action (Shao et al. 2004; Shao et al. 2010). A structural quantitative parameter was defined based on the void ratios of undistributed, remolded, and saturated loess under identical pressure and discussed the variations in the structural parameter relative to variations in pressure and moisture content (Chen et al. 2006).

Studies on the structural parameters of undisturbed loess mainly analyze its mechanical properties in the undisturbed, remolded, and saturated state to obtain its quantitative parameters. However, the structural parameters of undisturbed loess cannot be used to evaluate the structural properties of compacted loess, which are determined by changes in spatial arrangement, secondary bonding, and suction-induced cementation of particles

Editorial handling: Wissem Frikha

✉ Yan-zhou Hao
30010508@hncj.edu.cn

Tie-hang Wang
wagntx@xauat.edu.cn

Juan-juan Wang
juanjuan0022@163.com

[1] College of Civil Engineering, Xi' an University of Architecture and Technology, Beilin District Yanta Road No.13, Xi'an 710055, Shaanxi, China

during remolding and compaction. Based on the idea of comprehensive structural potential, Chen et al. (2014) compared the unconfined compressive strengths of compacted soil and saturated compacted soil, and thus defined the initial structural parameter, which is a quantitative index reflecting the maximum comprehensive structural potential when compacted loess starts to damage, the ratio of maximum stress of compacted loess to maximum stress of saturated compacted loess under the same axial strain, and the unconfined compression condition. Different loess initial moisture contents before compaction commonly influence structural properties of loess after compaction. While quantitative comparison and analysis of the structural properties of compacted loess and saturated compacted loess can represent the physical and structural state relative to saturated compacted loess, such comparison is inadequate in defining practical guidance for engineering of compacted loess, because it cannot represent the optimal structural state in which the samples have the maximum dry density and the optimal moisture content.

When tamping, rolling, and other methods are adopted to compact foundation and roadbed, the compaction processes and sample moisture content exert a significant influence on the structure of the compacted fine-grained soil (Seed and Chan 1959, Barden and Sides 1970), and an even more significant influence on soil mechanical properties (Gens 1995; Sivakumar and Wheeler 2000). Structural changes in compacted soil incurred by the initial moisture content before compaction exert a marked influence on compression properties and triaxial stress-strain characteristics of unsaturated compacted clay (Sivakumar et al. 2006; Vanapalli et al. 1999; Wang et al. 2009; Yin et al. 2012). However, existing literature has rarely investigated the structural properties of unsaturated compacted loess, especially the influence of structural properties on the matric suction and stress-strain characteristics of unsaturated compacted loess. Even though maximum dry density is an important physical index to evaluate soil compaction quality, it cannot reflect the influence of structural properties on the engineering properties of compacted soil. Therefore, this study conducts a soil-water characteristic curve test and a triaxial shear test on unsaturated compacted loess with different sample moisture contents to investigate the influence of structural changes incurred due to sample moisture content on the matric suction and stress-strain characteristics of unsaturated compacted loess. This paper proposes an engineering quality evaluation parameter that could reflect the structural properties of compacted loess.

Test overview

Materials

The soil sample used in this study was Q_3 Malan loess collected from Taiyi Road in Xi'an, China. Malan loess is yellowish brown, plastic, locally stiff-plastic, and slightly wet, with well-developed pores. Table 1 shows the physical properties of loess samples were determined following the Chinese National Standards GB/T50123-1999 (SAC 1999).

Soil samples from the soil layer were naturally air-dried and then pulverized with a rubber hammer which could separate the cemented particles only, but did not damage the loess particles. After that, the pulverized loess was sieved through a 2-mm mesh to prepare remolded soil samples with moisture content (w^0) of 14, 16, 18, and 20%. The compacted dry density was 1.7 g/cm^3. Next, the same moisture content (18%) was achieved through humidification or dehumidification. In this case, sample structures were composed of particles with different bonding and arrangements. Particles less than 0.005 mm in size accounted for 30.3% of soil samples, and clay particle content was relatively high, suggesting that the structure of unsaturated compacted loess samples was dominated by aggregation and cementation and that there were stable inlaid pores among aggregates (Table 1).

Testing techniques

Samples were prepared using a purpose-made sample press. Wet soil was weighed based on the calculation according to the dry density and moisture content, and was compacted in five layers. The samples for the soil-water characteristic test were cut out of the compacted loess using a cutting ring with an inner diameter of 70 mm and height of 19 mm. Sample dimensions were 70 mm in diameter and 19 mm high. Triaxial shear test samples were cut out using a soil cutting plate, and the dimensions of samples were 39.1 mm in diameter and 80 mm high (Fig. 1). The error in dry density was controlled to be ≤ 0.02 g/cm^3, and the error in moisture content was controlled to be $\leq 1\%$. In order to maintain the various structural properties, the moisture content of compacted soil samples was measured to bring the moisture content of all the soil samples to 18% through humidification or dehumidification. For samples with moisture content less than 18%, moisture content was increased to 18% using the syringe dripping method. For samples with moisture content greater than 18%, samples were air-dried to reduce moisture content to 18%. Once moisture content was brought to 18%, samples were wrapped with preservative film and were put inside a moisturizing cabinet for more than 48 h, so that they would have a homogenous moisture content distribution. The amount of water to be added/removed for humidification/dehumidification was calculated using Eq. (1):

$$m = \frac{m_0}{1 + 0.01 \times w_0} \times 0.01(w_1 - w_0) \quad (1)$$

where m represents the water mass to be added ($m > 0$)/removed ($m < 0$) (g); m_0 represents initial sample mass (g); w_0

Table 1 Main physical properties of loess

Relative density, G_S	Liquid limit, W_L (%)	Plastic limit, W_P (%)	Particle composition/%			
			> 0.075	0.075–0.01	0.01–0.005	< 0.005(mm)
2.71	30.7	18.4	3.2	49.7	16.8	30.3

represents sample moisture content (%); and w_1 represents the target moisture content (%).

Soil-water characteristic curve test

The soil-water characteristic curve test on unsaturated compacted loess adopted GEO-Experts (Mei et al. 2013) stress-related soil-water characteristic curve pressure plate apparatus (Fig. 2), and used a high air entry ceramic plate (5 bar). The high air entry ceramic plate has small pores of relatively uniform size. The plate acted as a membrane between air and water (Fig. 3). Once the plate was saturated with water, air could not pass through the plate due to the ability of the contractile skin to resist the flow of air. The ability of the ceramic plate to withstand the flow of air resulted from the surface tension of water, T_s, developed by the contractile skin which acted like a thin membrane joining the small pores of radius, R_s, on the surface of the ceramic plate. The difference between the air pressure above the contractile skin and the water pressure below the contractile skin was defined as matric suction. The maximum matric suction that was maintained across the surface of the plate was called its air entry value, $(u_a - u_w)_d$ (Fredlund and Rahardjo 1993). Each sample was tested at four different air pressures of 50 kPa, 100 kPa, 150 kPa, and 200 kPa. The next step was to prepare samples with moisture contents (w^0) of 14, 16, 18, and 20% with a dry density of 1.7 g/cm^3. Samples were humidified/dehumidified to achieve a moisture content of 18%, after that, saturated by vacuum with water. The ceramic plate was saturated with water, then the sample was put into the soil sample chamber, and the air pressure was applied to the soil sample to measure the mass of water discharged from the soil sample. Test data were recorded every 24 h for each air pressure level.

Triaxial shear test

Triaxial shear tests were performed using a strain-controlled triaxial apparatus, designed on the basis of Mohr-Coulomb strength theory to test the stress-strain relationship and shear failure strength of soil samples under different confining pressures (Fig. 4). The confining pressure was applied to the soil sample in the axial chamber by the confining pressure loading system, and the axial stress was applied to the soil sample by the axial loading system which could control the strain rate while keeping the confining pressure constant. With increasing deviator stress ($\sigma_1 - \sigma_3$), soil samples gradually reached the limit equilibrium state and shear failure occurred. Samples were tested for unconsolidated-undrained (UU) shear test (shear rate, 0.5 mm/min; confining pressures, 100 kPa, 200 kPa, and 300 kPa). The shear failure point was determined by the peak deviator stress ($\sigma_1 - \sigma_3$) on the stress-strain curve. When no peak value was present, the deviator stress ($\sigma_1 - \sigma_3$) corresponding to 15% axial strain was taken as the shear failure point, and the test was concluded when axial strain reached 19% (SAC 1999).

Analysis of test results

Influence of structural properties on the matric suction of unsaturated compacted loess

Soil-water characteristic curve tests are a time-consuming, complex, contain data discreteness, and the data measured by the test constitute only a portion of the soil-water characteristic curve. Therefore, an intact soil-water characteristic curve was developed by fitting the test data into Fredlund-Xing model (Fredlund and Xing 1994) given by:

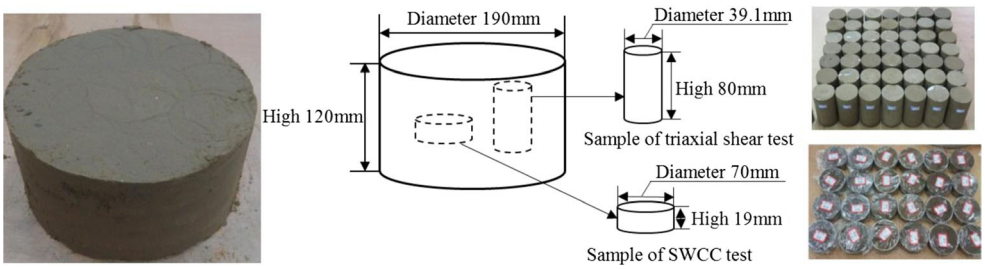

Fig. 1 Sample of compacted loess and schematic illustrations of test samples

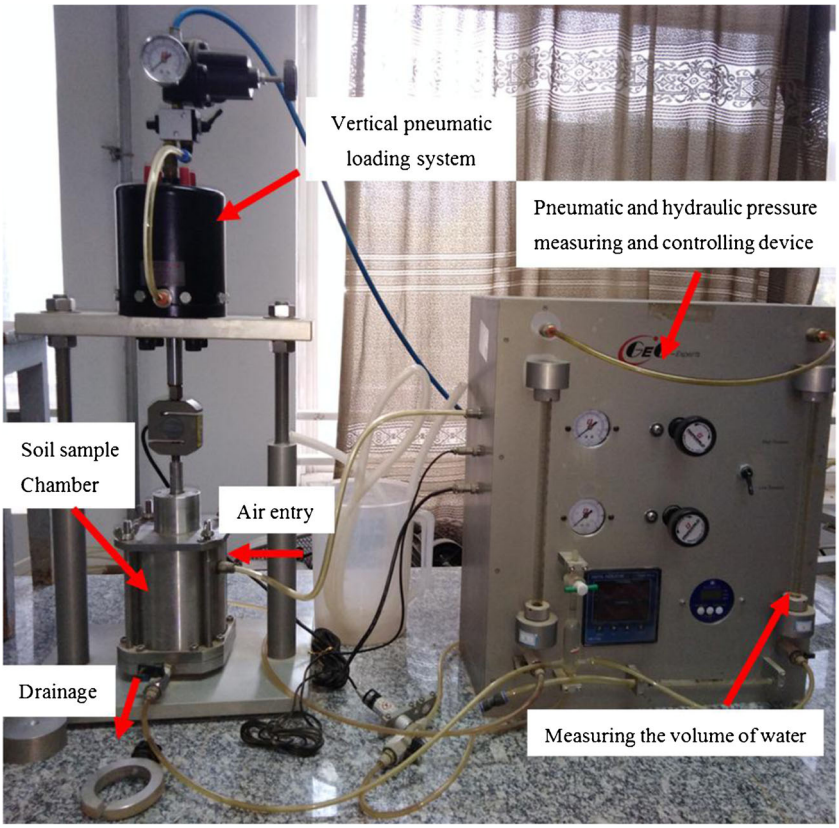

Fig. 2 GEO-Experts stress-related soil-water characteristic curve pressure plate apparatus

$$\theta = \frac{\theta_s}{\left\{\ln\left[e + \left(\frac{s}{a}\right)\right]^n\right\}^m} \quad (2)$$

where θ represents volumetric moisture content (%); θ_s represents saturated volumetric moisture content (%); s represents matric suction (kPa); e represents the base of natural logarithm ($e \approx 2.71828$); and a, m, and n represent model fitting parameters.

Fitting parameters obtained from Eq. (2) are shown in Table 2 and the fitting curve is shown in Fig. 5.

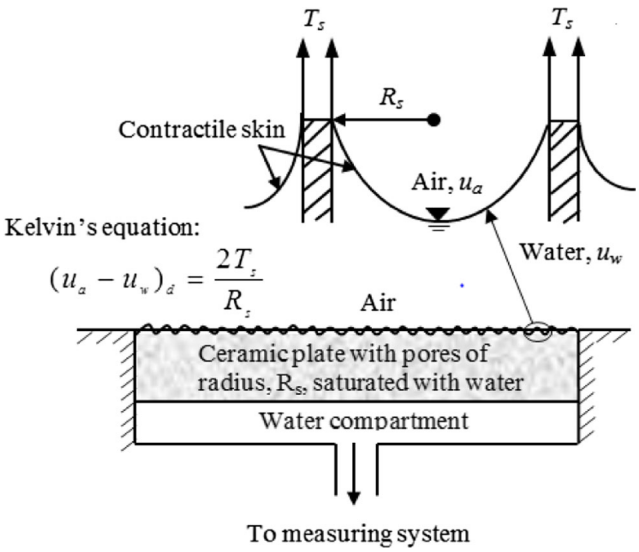

Fig. 3 Operating principle of a high air entry plate as described by Kelvin's capillary model (Fredlund and Rahardjo 1993)

(1). The soil-water characteristic curves obtained from tests for samples humidified/dehumidified to the same moisture content of 18% were markedly different. With increasing test moisture content, matric suction gradually decreased. With increasing matric suction, the slope of the soil-water characteristic curve gradually decreased, and the rate of moisture loss in soil samples gradually decreased as well. The structural properties of unsaturated compacted loess, caused by differences in sample preparation, exerted a significant influence on matric suction.

(2). When $w^0 = 18\%$, the soil matric suction was relatively high. According to laboratory compaction tests following the Chinese National Standards GB/T50123-1999 (SAC et al. 1999), the optimal soil sample moisture content was 18.2%, and the maximum dry density was 1.69 g/cm^3, indicating that sample moisture content (18%) was approximate to the optimal moisture content and also close to the plastic limit (18.4%) of the soil sample. Since sample moisture content was approximately equal to the optimal moisture content, the

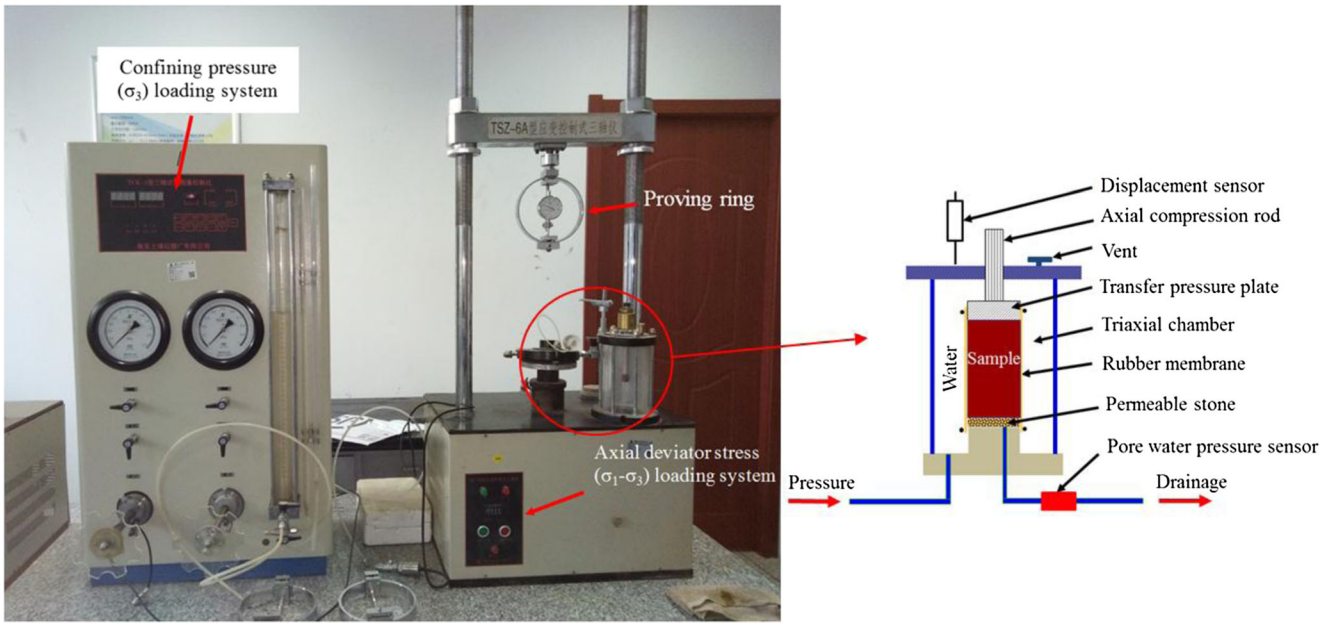

Fig. 4 Strain-controlled triaxial apparatus and schematic diagram of triaxial chamber

internal structure of the soil sample compacted to its maximum dry density and could be considered to be in the optimal structural state, in which case the matric suction of unsaturated compacted loess and strength were relatively high.

In order to further study the influence of sample moisture content (w^0) on matrix suction, the matrix suction values corresponding to three moisture content (test moisture content w) 16.5, 18.0, and 19.5% in the process of soil-water characteristic curve test were used to analyze the influence of sample moisture content (Fig. 6).

(1). At the same sample moisture content (w^0), the matric suction (s) of unsaturated compacted loess decreased markedly with increasing test moisture content (w). When $w^0 = 14\%$, the difference between the matric suction corresponding to $w = 16.5\%$ and that corresponding to $w = 19.5\%$ was 86.5 kPa; when $w^0 = 16\%$, it was 98.1 kPa; when $w^0 = 18\%$, that was 109.6 kPa; and when $w^0 = 20\%$, it was 81 kPa. For $w^0 = 18\%$, the test moisture content difference was only 1.5% ($\Delta w =$ 18.0%–16.5%), and the matric suction difference could reach as high as 63.4 kPa ($\Delta s = 178.8$ kPa − 115.4 kPa).

(2). For a given test moisture content (given that sample moisture content did not exceed the plastic limit, i.e., 18.4% of the soil sample), matric suction approximately increased linearly with increasing sample moisture content. When the soil sample was compacted at relatively low sample moisture content, the water in the soil was primarily combined with soil particles in the form of bound water. The water film on the surface of soil samples was relatively thin, and the soil sample contained a lot of gas thereby having a poor water-holding capacity. However, when sample moisture content was approximately equal to the plastic limit, soil samples had relatively larger and more inhomogeneous pores for the same compacted dry density. Thus, when sample moisture content was relatively low, suction was relatively low as well.

(3). When sample moisture content ($w^0 = 18\%$) was close to the optimal moisture content ($w^0 = 18.2\%$), the soil samples displayed an aggregation structure and had relatively small homogeneous pores. Accordingly, soil samples

Table 2 Fitting parameters of Fredlund-Xing equation

Sample moisture content, w^0/%	Dry density, ρ_d (g/cm^3)	Fitting parameter				
		θ_s (%)	a	n	m	R^2
14	1.7	36.9026	38.2522	2.3343	0.2329	0.9929
16	1.7	36.9094	43.3692	2.1082	0.2559	0.9910
18	1.7	37.1018	51.1416	1.8381	0.3019	0.9909
20	1.7	36.9197	37.3552	2.5025	0.2314	0.9911

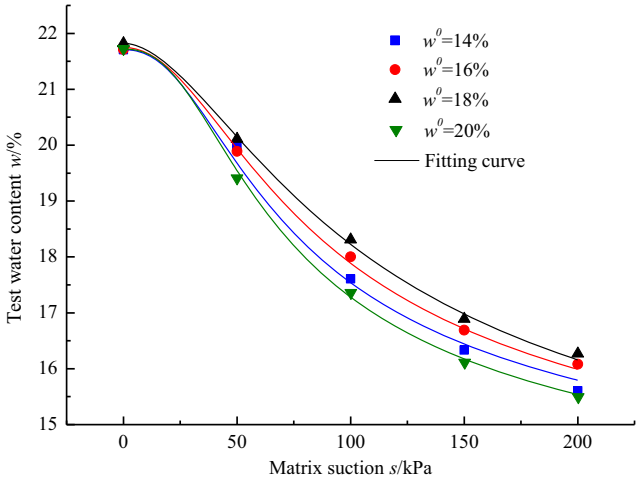

Fig. 5 Soil-water characteristic curve

had a relatively high air entry value, and because of draining difficulties, samples also had a relatively good water-holding capacity and a relatively high suction.

(4). When sample moisture content ($w^0 = 20\%$) exceeded the optimal moisture content, the water film thickened, and the moisture in soil gradually transformed into free water. When moisture content was relatively high, the difference between the potential energy of pore water and that of free water was relatively small, resulting in relatively low suction (zero when saturated).

Influence of structural properties on the stress-strain characteristics of compacted loess

Triaxial shear tests were conducted to obtain the stress-strain curves shown in Fig. 7.

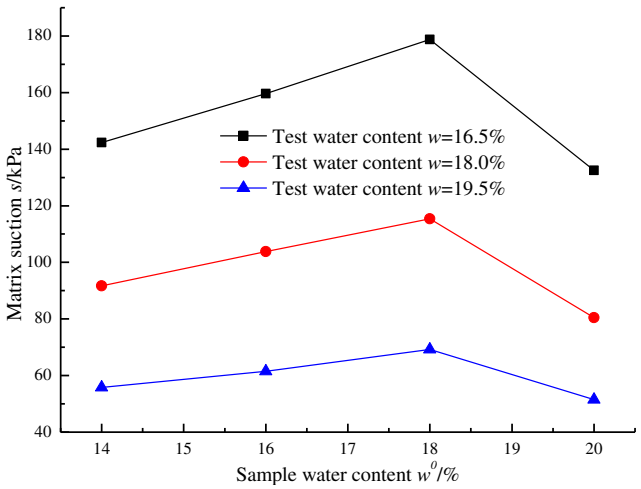

Fig. 6 Relation curve between sample moisture content and matric suction

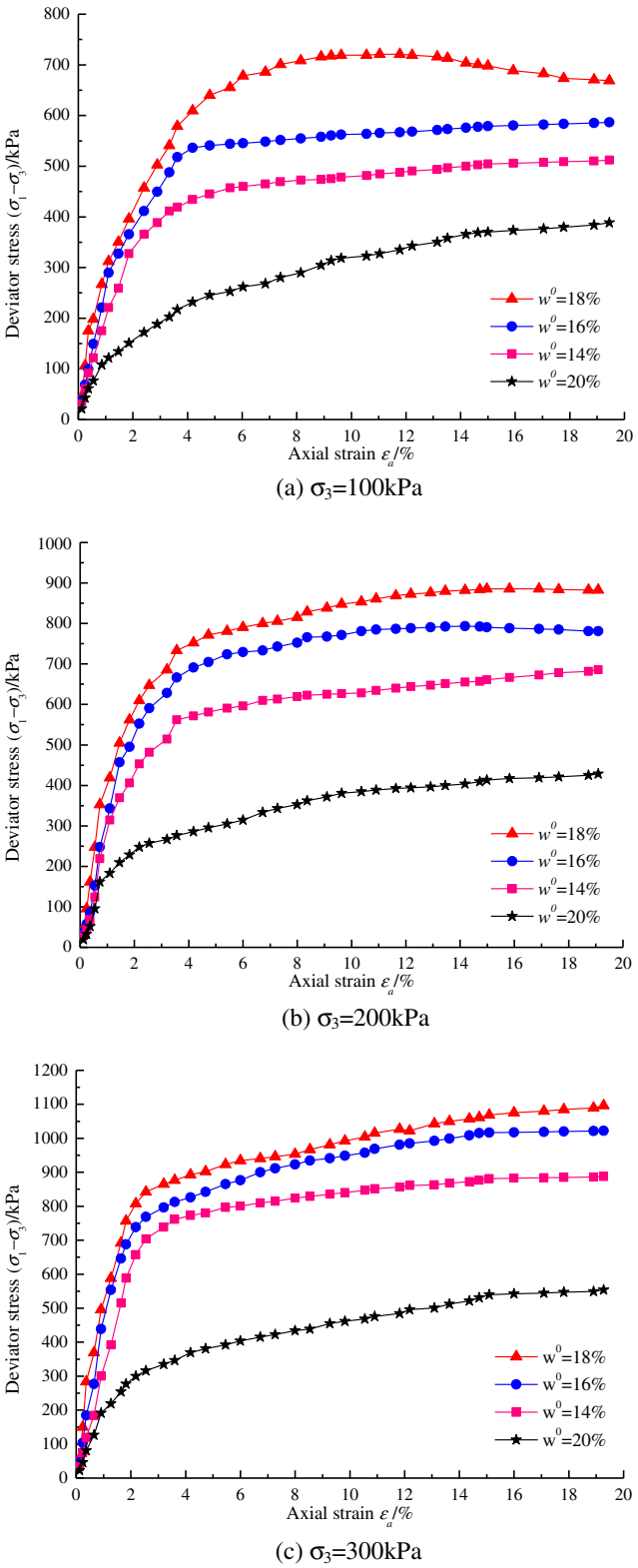

Fig. 7 Stress-strain curves of unsaturated compacted loess of different sample moisture contents

(1). Stress-strain curves obtained from the triaxial shear test at different sample moisture contents differed quite significantly. The curve corresponding to a sample

moisture content of 18% was located at the top, with the highest deviator stress. The stress-strain curve corresponding to a sample moisture content of 20% differed most significantly from the other three stress-strain curves and had the lowest deviator stress. During the change in stress-strain curves from high to low in the $(\sigma_1-\sigma_3)-\varepsilon_a$ coordinate, the corresponding of sample moisture contents were respectively 18, 16, 14, and 20%.

(2). Stress-strain curves for soil samples with different sample moisture contents showed plastic failure types of weak softening and weak hardening under different confining pressures. While the stress-strain curve corresponding to $w^0 = 18\%$ was weak softening type, the stress-strain curve had a peak value, which was not obvious when the confining pressure was 100 kPa, and the shear failure point was determined by the peak value. All the other stress-strain curves were weak hardening type, in which the deviator stress increased gradually with increasing axial strain, and shear failure points were determined by the corresponding values at 15% axial strain (SAC et al. 1999 and ASTM 2011).

(3). The linear stage of the stress-strain curve was obvious under each confining pressure. The stress-strain curves corresponding to $w^0 = 14\%$, $w^0 = 16\%$, and $w^0 = 18\%$ were linear for different confining pressures when axial strain $\varepsilon_a \le 2\%$, and their slopes increased with increasing confining pressure. When axial strain $\varepsilon_a > 2\%$, stress-strain curves showed nonlinear characteristics. The stress-strain curve for $w^0 = 20\%$ was linear when axial strain $\varepsilon_a \le 1\%$, and nonlinear when axial strain $\varepsilon_a > 1\%$.

(4). In an ideal state, the stress-strain curves of soil samples with the same dry density and moisture content should be consistent under the same confining pressure. However, the differences shown in the above test results were significant, which attributed to the different structural properties of compacted loess. Structural properties primarily include the spatial arrangement, secondary bonding, and suction cementation of particles formed due to the remolding and compaction of loess (Chen et al. 2014).

(5). In the process of humidification of soil samples to bring the moisture content to 18%, pore water in soil gradually increased. When sample moisture content was relatively low (for instance, $w^0 = 14\%$), the soil sample had a large amount of pore space (mainly consisting of large- and medium-sized pores), hence the cementation among particles was relatively weak, and the suction was relatively low. Attraction among particles decreased with the gradual thickening of the water film on the surface of clay particles. In the case of triaxial shear failure, the resistance to failure was relatively low, and the deviator stress was relatively small. With an increase in sample moisture content (for instance, $w^0 = 16\%$) (still below the optimal moisture content of 18.2%), the content of high- and medium-sized pores gradually decreased during the compaction process; however, the content of micro-pores, especially stable inlaid pores, gradually increased. With increasing number of clay particles of the same volume, there was an increase in the water film area on particle surfaces, thinning of the water film, as well as attraction among particles. The arrangement of soil particles, dominated by aggregates, became more compact and was accompanied by gradual increasing cementation among particles and suction. The deviator stress increased in the triaxial shear test.

(6). When sample moisture content ($w^0 = 18\%$) was close to the optimal moisture content ($w = 18.2\%$), soil samples exhibited an aggregation structure dominated by relatively small stable inlaid pores with a homogeneous distribution. Matric suction was also relatively high, the secondary bonding formed in the soil had the maximum strength, and the soil particle arrangement had the highest degree of compaction. In this case, soil samples were in the optimal structural state, and the deviator stress was highest when soil samples failed in the triaxial shear test.

(7). When sample moisture content ($w^0 = 20\%$) exceeded the optimal moisture content, the attraction among clay particles decreased due to the relatively thick water film on the surface of soil particles. Inter-particle pores were relatively large, and suction was relatively low. During the dehydration process, inter-particle pores gradually expanded, which was accompanied by a significant reduction in structural strength. In this case, the deviator stress was the lowest.

Variation in structural parameters of unsaturated compacted loess during triaxial shear

After humidifying (or dehumidifying) soil samples to the optimal moisture content of 18% and compacting them until they reached the maximum dry density of 1.7cm^3, the stress-strain curves of soil samples were markedly different owing to the influence of changes in structural properties. This suggested that the optimal moisture content and the maximum dry density index could not reflect the structural properties of compacted loess. For this reason, after compacting soil samples to the maximum dry density (sample moisture content being equal to the optimal moisture content), the structural state of compacted loess was adopted as the optimal structural state. The triaxial shear

deviator stress $(\sigma_1 - \sigma_3)_y$ of soil samples at the optimal structural state was then compared with the deviator stress $(\sigma_1 - \sigma_3)_r$ of soil samples for other sample moisture contents compacted to the same dry density under the same axial strain ε_a. Hence, this paper defined a relative structural quantitative parameter $m_{\varepsilon r}$ that could reflect the influence of the structural properties on compacted soil. The equation is as follows:

$$m_{\varepsilon r} = \frac{(\sigma_1 - \sigma_3)_y}{(\sigma_1 - \sigma_3)_r} \tag{3}$$

Equation (3) was used to determine the relative structural parameter of compacted loess in the triaxial shear process, which could comprehensively reflect the influence of structural properties on compacted soil. The relative structural parameter is such that for soil compacted to the maximum dry density at the optimal moisture content, $m_{\varepsilon r} = 1$. In this paper, the corresponding deviator stress of $w^0 = 18\%$ was taken as $(\sigma_1 - \sigma_3)_y$, because $w^0 = 18\%$ was close to the optimal moisture content ($w = 18.2\%$).

Figure 8 shows the relationship between the relative structural parameter $m_{\varepsilon r}$ and axial strain ε_a.

(1). When $w^0 < 18\%$, with a decrease in w^0, the $m_{\varepsilon r} - \varepsilon_a$ curve gradually departed from the transverse axis, and the difference between the structural properties of compacted soil and soil in the optimal structural state gradually increased, mainly manifested by the differences in the size of inter-particle pores and the magnitude of suction. When $w^0 = 14\%$, the soil was dominated by large and medium-sized pores, which was contrary to the optimal structural state dominated by micro-pores, and the corresponding difference in suction was illustrated in Fig. 6. For a given volume of micro-particles, differences in clay particle content resulted in a relatively significant difference in attraction among clay particles. Thus, the $m_{\varepsilon r} - \varepsilon_a$ curve corresponding to $w^0 = 14\%$ showed a greater $m_{\varepsilon r}$ value in comparison to that the curve corresponding to $w^0 = 18\%$. When $w^0 = 16\%$, the soil experienced a transition from large and medium-sized pores to micro-pores. The difference from the optimal structural state in terms of pore size decreased, and the corresponding difference in suction was relatively small. In same-volume of micro-particles, the difference in clay particle content decreased, accompanied by a decreased difference in clay particle attraction. Thus, the $m_{\varepsilon r} - \varepsilon_a$ curve corresponding to $w^0 = 16\%$ presented a smaller $m_{\varepsilon r}$ value in comparison to the curve corresponding to $w^0 = 14\%$.

(2). When $w^0 = 18\%$ (close to the optimal moisture content $w = 18.2\%$), the corresponding deviator stress $(\sigma_1 - \sigma_3)$

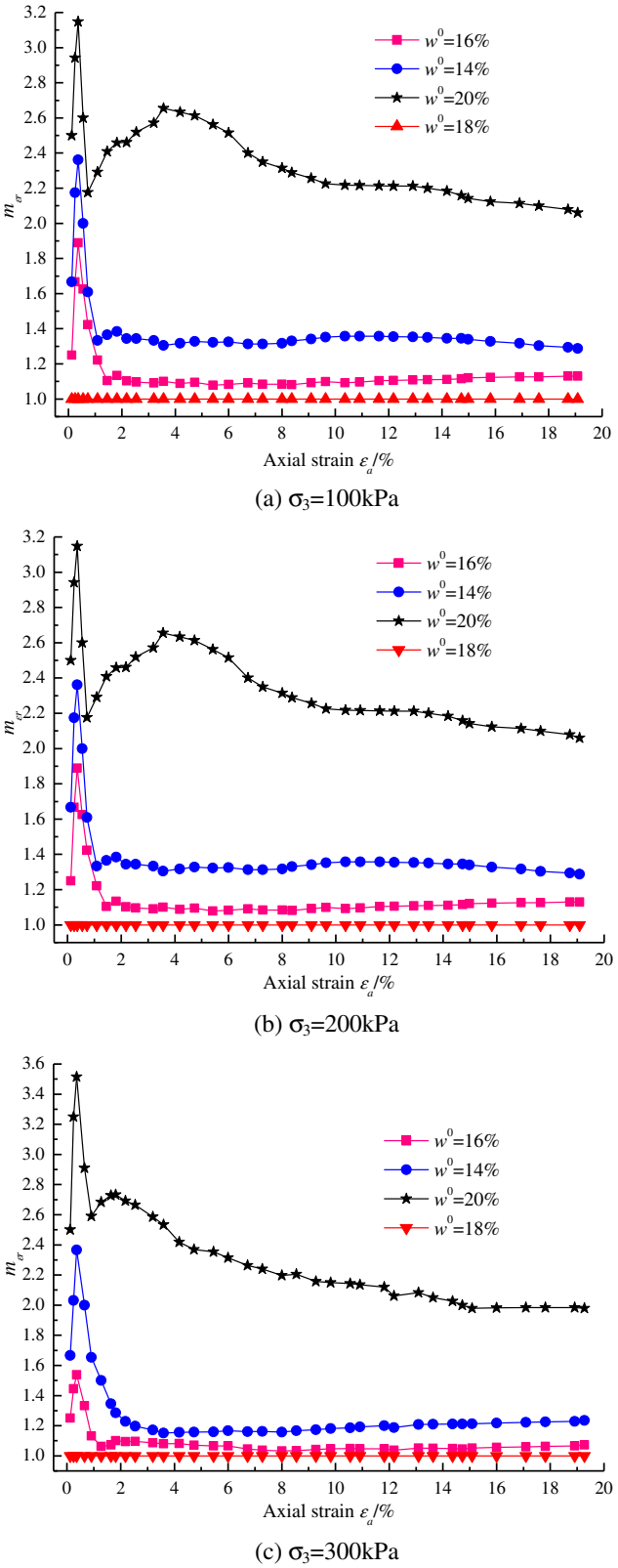

Fig. 8 Relationship curves between the relative structural parameter $m_{\varepsilon r}$ and axial strain ε_a of unsaturated compacted loess of different sample moisture contents

was taken as $(\sigma_1 - \sigma_3)_r$ which equaled approximately to $(\sigma_1 - \sigma_3)_y$, $m_{\varepsilon r} \approx 1$. The $m_{\varepsilon r} - \varepsilon_a$ curve was a straight line parallel to the transvers axis.

(3). When $w^0 = 20\%$, the $m_{\varepsilon r} - \varepsilon_a$ curve was farther away from the top of the transverse axis, the difference between the structural properties of soil samples and those in the optimal structural state increased, and the $m_{\varepsilon r}$ value was largest. This was caused by the expanded pores and decreased suction during the dehydration process. In the triaxial shear test, soil sample moisture content was always 18%, hence the cementation states among soil particles were close.

(4). The characteristics of $m_{\varepsilon r} - \varepsilon_a$ curve corresponding to various sample moisture contents were similar, which manifested an obvious regularity. When $\varepsilon_a < 1.2\%$, with increasing axial strain ε_a, $m_{\varepsilon r}$ began to gradually increase to its peak, after which it began to decrease. When $\varepsilon_a \approx 0.5\%$, $m_{\varepsilon r}$ values were largest, and the structural difference in the linear stage reached its maximum, suggesting that the structural properties manifested by compacted soil in this case were more significant. When $\varepsilon_a = 1.2\%$, various $m_{\varepsilon r} - \varepsilon_a$ curves showed that $m_{\varepsilon r}$ values decreased from the peak value to its minimum value, and the structural difference in the linear stage of the corresponding stress-strain curve reached a minimum. When $\varepsilon_a = 2\%$, $m_{\varepsilon r} - \varepsilon_a$ curves corresponding to $w^0 = 14\%$ and $w^0 = 16\%$ had relatively small peak values, and in those cases, the linear stage of the corresponding stress-strain relation curve began to transition to the nonlinear stage, in which the corresponding $m_{\varepsilon r0}$ was defined as the yielding structural parameter. When $\varepsilon_a > 2\%$, the $m_{\varepsilon r} - \varepsilon_a$ curve tended to be gentle.

(5). Confining pressure had marked influence on the characteristics of the $m_{\varepsilon r} - \varepsilon_a$ curve. The peak $m_{\varepsilon r}$ corresponding to $\varepsilon_a \approx 0.5\%$ increased with increasing σ_3. When $\sigma_3 = 100$ kPa, 200 kPa and 300 kPa, $m_{\varepsilon r}$ values were 2.88, 3.18 and 3.50, respectively. When $\varepsilon_a > 0.5\%$, $m_{\varepsilon r}$ decreased with increasing σ_3, and $m_{\varepsilon r} - \varepsilon_a$ curve gradually approached ε_a axis with an increase in σ_3. The structural properties of compacted loess weakened with increasing confining pressure.

(6). When the $m_{\varepsilon r} - \varepsilon_a$ curve approached $m_{\varepsilon r} \approx 1$, the structural properties were approximately equal to those in the optimal structural state, and the compaction quality of the compacted soil increased. The $m_{\varepsilon r} - \varepsilon_a$ curve could reflect the structural properties of the linear stage of the stress-strain curve for different w^0 values, especially the transition from the linear to nonlinear stage, suggesting that structural parameter $m_{\varepsilon r}$ could better reflect the influence of structural changes incurred due to varying sample moisture content of compacted loess.

Conclusions

By conducting soil-water characteristic curve tests and triaxial shear tests on unsaturated compacted loess with varying structural properties after humidifying (or dehumidifying) samples to the same moisture content and compacting samples to the same dry density, this study investigated the influence of structural properties on matric suction and the stress-strain relationship of unsaturated compacted loess and drew the following conclusions:

(1). Structural changes incurred from varying sample moisture content markedly influenced the soil-water characteristic curve of unsaturated compacted loess. When sample moisture content was smaller than the optimal moisture content, the matric suction increased with increasing sample moisture content. At the optimal sample moisture content, unsaturated compacted loess exhibited a homogeneous micro-pore aggregation structure, and had relatively high suction. When sample moisture content was greater than the optimal moisture content, matric suction decreased rapidly.

(2). The stress-strain curves for compacted loess samples with different sample moisture contents were mostly of the weak hardening type under different confining pressures. Stress-strain curves presented significant differences due to the influence of structural properties. The stress-strain curve for soil in the optimal structural state was located at the top end. When sample moisture content was below the optimal sample moisture content, the degree of structural weakening was relatively low, and its stress-strain curve gradually moved down. When sample moisture content was greater than the optimal sample moisture content, the degree of structural weakening in the soil sample was relatively high, and the stress-strain curve was located at the bottom of the graph.

(3). The structural state of compacted loess at the optimal sample moisture content was adopted as the optimal structural state and a relative structural quantitative parameter $m_{\varepsilon r}$ was defined. Results showed that this parameter could reasonably reflect the structural properties of compacted soil, and make up for the deficiency of the optimal moisture content and maximum dry density index in reflecting the influence of structural properties.

(4). The structural properties of unsaturated compacted loess are of great significance and seriously impact the quality of compacted soil engineering. Thus, in practical engineering, it is necessary to sample soil layers which have been compacted for a long period, conduct triaxial shear testing of samples, and compare the deviator stress $(\sigma_1 - \sigma_3)_r$ with the deviator stress $(\sigma_1 - \sigma_3)_y$ obtained from triaxial shear test on the samples which were compacted

under the optimal moisture content and the maximum dry density in laboratory, then calculate the $m_{\varepsilon r}$ according to Eq. (3). The engineering quality of compacted loess is determined by whether the value of the $m_{\varepsilon r}$ is close to one. When the $m_{\varepsilon r}$ is close to one, the compacted loess has the highest strength and minimum compression deformation, and when the $m_{\varepsilon r}$ is greater than one, the engineering quality of compacted loess is poor.

Acknowledgements This study was supported by the Fund Program for the National Natural Science Foundation of China, Special Scientific Project of Shaanxi Education Department of China.

The authors would like to thank to the team members of the key discipline of geotechnical engineering and the workers of the geotechnical engineering laboratory.

Funding information This work was supported by the National Natural Science Foundation of China (No. 51078309) and Special Scientific Project of Shaanxi Education Department of China (No. 16JK1448).

References

ASTM (2011) D2850–15: standard test method for unconsolidated-undrained triaxial compression test on cohesive soils, vol 04.08. West Conshohocken, Pennsylvania

Barden L, Sides GR (1970) Engineering behavior and structure of compacted clay. Journal of Soil Mechanics and Foundation Engineering 96(4):1171–1200

Chen CL, Hu ZQ, Gao P (2006) Research on relationship between structure and deformation property of intact loess. Rock Soil Mech 27(11):1891–1896

Chen CL, Jiang X, Su TZ, Jin J, Li WW (2014) The influence of structure on unconfined compression characteristics of compacted loess. Chin J Rock Mech Eng 33(12):2539–2545

Fredlund DG, Rahardjo H (1993) Soil mechanics for unsaturated soils. Wiley, New York, pp 97–98

Fredlund DG, Xing A (1994) Equation for the soil-water characteristic curve. Can Geotech J 31(4):521–532

Gens A (1995) Constitutive modeling: application to compacted soils. In: Proceedings of the 1st international conference of unsaturated soils, Paris, pp 1179–1200

Mei L, Jiang PM, Li P, Zhou AZ (2013) Soil-water characteristic curve tests on unsaturated soil. Chin J Geotech Eng 35(1):124–128

Seed HB, Chan CK (1959) Structure and strength characteristics of compacted clays. J Soil Mech Found Eng 85(5):87–128

Shao SJ, Zhou FF, Long JY (2004) Structural properties of loess and its quantitative parameter. Chin J Geotech Eng 26(4):531–536

Shao SJ, Zheng W, Wang ZH, Wang S (2010) Structural index of loess and its testing method. Rock Soil Mech 31(1):15–19

Shen ZJ (1996) The mathematical model for the structured soils. Chin J Geotech Eng 18(1):95–97

Sivakumar V, Wheeler SJ (2000) Influence of compaction procedure on the mechanical behaviour of an unsaturated compacted clay. Geotechnique 50(4):359–368

Sivakumar V, Tan WC, Murray EJ, Mckinley JD (2006) Wetting, drying and compression characteristics of compacted clay. Geotechnique 56(1):57–62

Standardization Administration of China (SAC), Ministry of Water Resources (1999) China National Standards GB/T50123–1999: standard for soil test method. Beijing 100–106

Vanapalli SK, Fredlund DG, Pufahl DE (1999) The influence of soil structure and stress history on the soil-water characteristics of a compacted till. Geotechnique 49(2):143–159

Wang DL, Luan MT, Yang Q (2009) Experimental study of soil-water characteristic curve of remolded unsaturated clay. Rock Soil Mech 30(3):751–756

Xie DY, Qi JL (1999) Soil structure characteristics and new approach in research on its quantitative parameter. Chin J Geotech Eng 21(6): 651–656

Yin PP, Niu SK, Wei CF (2012) Effect of dry density and initial moisture content on soil-water characteristic curve of remolded unsaturated silt. Hydrogeol Eng Geol 39(1):42–46